

Praktikum: P4 Gruppe: 22

☒ **Mo** ☐ **Mi**
Zutreffendes bitte ausfüllen

WS20/21

Namen: Paul Filip useba[at]student.kit.edu

Namen: Janic Beck

Versuch: Comptoneffekt

Betreuer: Roxanne Turcotte Durchgeführt am: 16.11.20

Wird vom Betreuer ausgefüllt.

1. Abgabe am: _____

Rückgabe am: _____ Kommentar: _____

2. Abgabe am: _____

Ergebnis: + / 0 / - Handzeichen: _____

Datum: _____ Kommentar: _____

Contents

2. Theory & Preparation

2.1 Compton scattering

Consider the scenario of a high-energy photon interacting with an unbound electron as shown in ???. To describe this process we choose a coordinate frame where the electron is at rest with respect to us. In the experiments to be presented in this report such a coordinate frame conveniently is the lab frame anyways. Furthermore, we employ natural units, $\epsilon_0 = \hbar = c = 1$.

From the conservation of energy and impulse we can construct a theoretical description of this process based on the initial and final energies of both particles.

$$\begin{aligned} E_{\gamma,i} + \underbrace{E_{e,i}}_{=0} &= E_{\gamma,f} + E_{e,f} \\ p_{\gamma,i} + \underbrace{p_{e,i}}_{=0} &= p_{\gamma,f} + p_{e,f} \end{aligned}$$

From the above relations an expression for the energy of the photon after interacting with the electron can be obtained as lined out in [?]. It reads

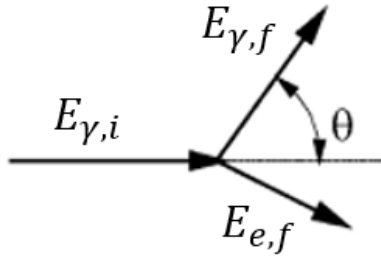
$$E_{\gamma,f} = \frac{E_{\gamma,i}}{1 + \frac{E_{\gamma,i}}{m_e}(1 - \cos \theta)}, \quad (2.1)$$

where θ defines the angle spanned between the incident photon and its path post scattering. It follows that the electron gains energy from the interaction.

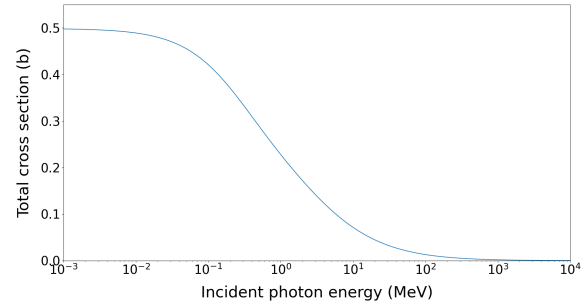
$$E_{e,f} = E_{\gamma,i} - E_{\gamma,f} = E_{\gamma,f} \cdot \frac{E_{\gamma,i}}{m_e} \cdot (1 - \cos \theta). \quad (2.2)$$

The measureable change in the photons wavelength $\lambda = \frac{hc}{E_{\gamma}}$ due to the interaction is called the **Compton effect**. The underlying elastic scattering of photons and unbound electrons is consequently labelled **Compton scattering**. Alongside Photoionisation and Pair production it represents one of the important processes by which electromagnetic radiation interacts with matter.

The physical characteristics of Compton scattering, namely its cross section and the resulting distribution of electron energies will be discussed in the following ?? and ??.



(a) Scattering kinematics



(b) Total cross section

(a) A high energy photon scatters off a free electron at rest. The defining variables to describe this process are given by $E_{\gamma,i}$ and θ . Figure adapted with changes from [?]. (b) The total cross section as a function of the incident photon energy. Roughly constant for low-energy photons, the total cross section drops off quickly for higher energies.

2.2 Cross section

Compton scattering is the dominating effect by which photons with an energy between 100 keV and 10 MeV interact with matter [?]. A theoretical description of the processes cross section is given by the **Klein-Nishina formula** (KN).

$$\frac{d\sigma}{d\Omega}_{\text{KN}} = \frac{\alpha^2}{2m_e} \left(\frac{E_{\gamma,f}}{E_{\gamma,i}} \right)^2 \left[\frac{E_{\gamma,f}}{E_{\gamma,i}} + \frac{E_{\gamma,i}}{E_{\gamma,f}} - \sin^2 \theta \right] \quad (2.3)$$

Integrating over all solid angles and defining $x = \frac{E_{\gamma,i}}{m_e}$, one obtains the total cross section.

$$\sigma_{\text{tot.}} = \int \frac{d\sigma}{d\Omega} d\Omega = \frac{\pi\alpha^2}{m_e^2} \frac{1}{x^3} \left(\frac{2x(2 + x(1+x)(8+x))}{(1+2x)^2} + ((x-2)x - 2 \log(1+2x)) \right) \quad (2.4)$$

In the low-energy limit of $x \ll 1$?? simplifies to a constant called the **Thomson cross section**, whereas in the high-energy limit $x \rightarrow \infty$ we expand in x to find that the cross section vanishes. This behaviour can also be seen in ??.

$$\begin{aligned} x \ll 1 : \quad \sigma_{\text{tot.}} &= \frac{8\pi\alpha^2}{m_e^2} \approx 0.6652 \text{ b} \\ x \rightarrow \infty : \quad \sigma_{\text{tot.}} &= \frac{\pi\alpha^2}{xm_e^2} \left(\frac{1}{2} + \log 2x \right) \end{aligned}$$

Naively, one would therefore expect Compton scattering to be an important process for low to intermediate energy ranges of the electromagnetic spectrum, where the cross section $\sigma_{\text{Tot.}}$ is non-negligible. This is however not the case. Various other processes such as the photoelectric effect or Rayleigh scattering dominate the low energy regime and render Compton scattering only a fringe case. With higher photon energies, the cross section for the aforementioned processes drop off, and increase the importance of Compton scattering for gammas carrying an energy of 100 keV up to 10 MeV .

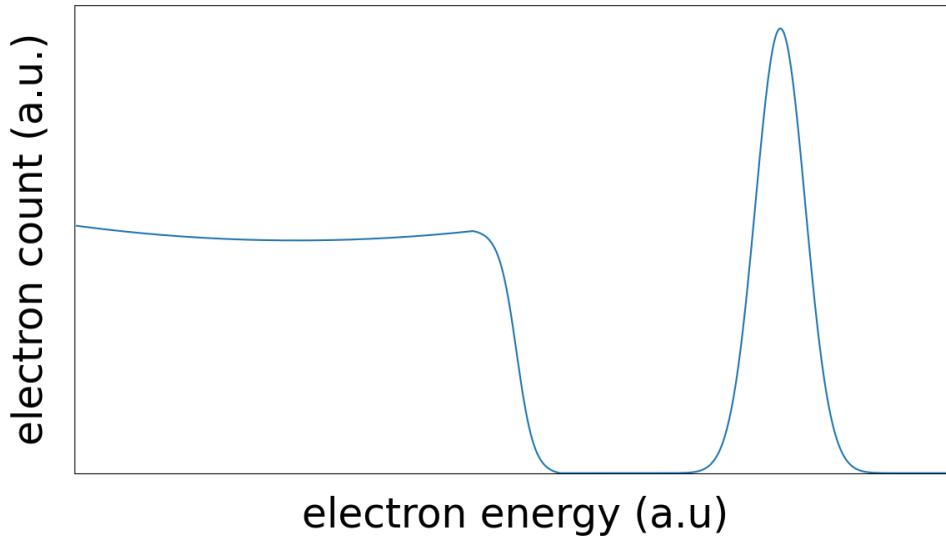


Figure 2.2: An idealised Compton spectrum. A relatively constant flux of electrons is measured up to an energy of E_{\max} , where the spectrum sharply drops off. At the high-energy end of the spectrum a gaussian shaped photopeak is visible.

2.3 Compton spectrum

Without knowing anything about the distribution of energies or deflection angles of the scattered electrons, by examining ?? it can already be established that the energy the electron gains from the interaction is directly proportional to $(1 - \cos \theta)$, or in other words, by how much the photon is scattered away from its original path. It follows that for $\theta = 180^\circ$ the electron gains a maximum energy of

$$E_{\max} = \frac{E_\gamma}{1 + \frac{m_e c^2}{E_\gamma}}. \quad (2.5)$$

Since the photon physically cannot dump more energy by this process, a sharp drop in the Compton spectrum at E_{\max} is expected. This characteristic drop-off is commonly called the **Compton edge**. Energetically lower than this cutoff lays the **Compton continuum**, or main part of the spectrum. Over a wide range of energies that correspond to scattering angles $\theta \in [0^\circ, 180^\circ]$ the flux of electrons remains approximately constant. This follows directly from ??.

Lastly, an idealised Compton spectrum as depicted in ?? will also display a characteristic **photopeak**. This photopeak is caused by photons directly interacting with detector material via the photoelectric effect. In this case, the entire energy of the photon is dumped inside the detector. It is therefore a helpful reference point for calibrations, albeit not being part of the Compton spectrum itself.

The measured Compton spectrum discussed in ?? will display several other characteristics such as a prominent X-ray line or a backscatter peak. These properties are dependant on the experimental setup. As such they will be discussed in the appropriate sections of ??.

3. Experiment & Evaluation

ToDo [W]rite up something about the experimental setup

3.1 Calibration of a multichannel analyser

As a first task the MAC needs to be calibrated so that measured channel numbers of an event can be related to the energy of the particles that caused it. The presented calibration is fourfold. In separate measurements the radionuclides Cobalt-57, and -60, as well as Sodium-22, and Caesium-137 are placed in front of the NaJ-scintillator. Their γ -spectrum is measured for 300 s. The resulting distribution of observed events across the different measuring channels is depicted in ???. The interesting parts of the spectra are the gaussian shaped sections located at the tail ends. They represent the photopeaks discussed briefly in ???.

ToDo Equipped with theoretical knowledge of the radioactive processes, one can compare the measured channel with the expected energy of a nuclear transition (see [??app:transitions]) to establish a linear connection between the two. For a more solid result this calibration is done simultaneously for all measured radionuclides. A linear regression over all reference points then allows a quantitative analysis of measurement results. Below listed in ??? are the different observed radioactive transitions, their characteristic transition energies, as well as the channel they were observed in by the MAC, the last column holds information about the location of a gaussian fit applied to the signal. In the bottom plot of ??? these results are furthermore visualised.

As can be seen both in the plot as well as the table, a calibration for the photopeaks of ^{60}Co are not conducted. From the location of other photopeaks the characteristic points of the ^{60}Co γ spectrum should be located around channels #195 and #223. This can however not be experimentally verified. A reasonable analysis cannot be completed, as the photopeaks are - provided the presented methodology is sound - far too faint. This can perhaps be prevented in future lab assignments by gathering more data of the ^{60}Co spectrum.

In any case, a linear model that connects channel number \mathcal{C} to a particle energy E is obtained. They can be related to each other via ??? that is presented below.

Table 3.1: MAC energy calibration parameters

Transition	Energy (keV)	measured channel	fit channel
$^{57}\text{Co} \rightarrow ^{57}\text{Fe}$	122.061	16	15.3(1)
$^{22}\text{Na} \rightarrow ^{22}\text{Ne}$	546.544	91	90.8(4)
$^{137}\text{Cs} \rightarrow ^{137m}\text{Ba}$	661.659	108	106.0(3)
$^{60}\text{Co} \rightarrow ^{60}\text{Ni}^*$	1173.200	-	see text
$^{60}\text{Ni}^* \rightarrow ^{60}\text{Ni}$	1332.000	-	see text

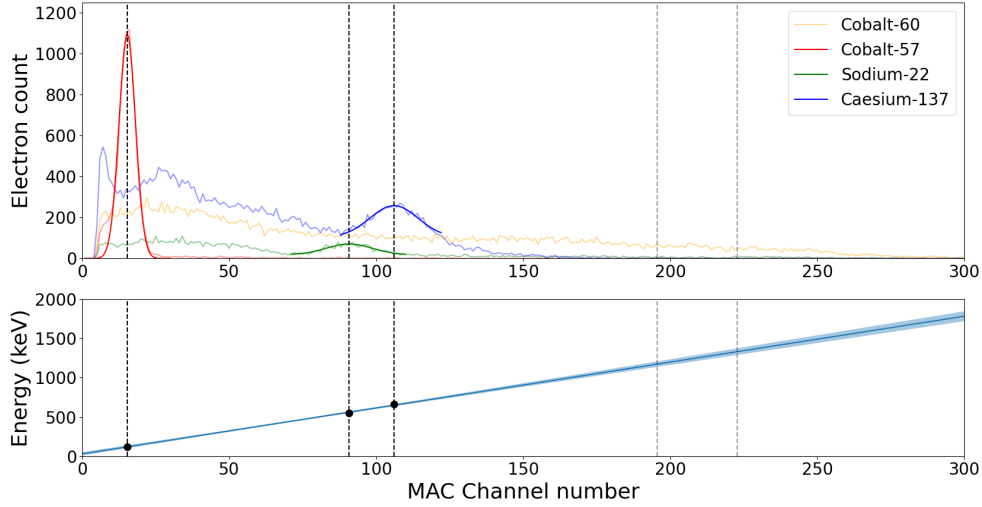


Figure 3.1

The gamma spectra of various radionuclides as measured by the MAC is depicted in the upper plot. A Gaussian fit highlights the characteristic photopeaks for each (except Co-60, see text) measurement. The lower plot sets the measured channel numbers into context with the energies of the observed transitions. A linear model that connects MAC channel number with an energy is established.

$$E(\mathcal{C}) = \underbrace{(5.8 \pm 0.3) \text{ keV}}_a \cdot \mathcal{C} + \underbrace{(30.2 \pm 22.0) \text{ keV}}_b \quad (3.1)$$

Albeit only three of the four radionuclides can be used effectively for a calibration, the results nevertheless seem promising. A quick check regarding the goodness of fit finds a reduced $\chi^2_\nu \approx 0.97$, indicating that the model conforms with observations to reasonable accuracy. This accuracy $\Delta E(\mathcal{C})$ can then be quantified using the covariance matrix $\text{COV}(a, b)$, estimated by the fitting algorithm, as well as the gradient ∇E , which can easily be calculated by hand.

$$\text{COV}(a, b) = \begin{bmatrix} 0.0736 & -5.2014 \\ -5.2014 & 483.5527 \end{bmatrix}, \quad \nabla E = \begin{pmatrix} \mathcal{C} \\ 1 \end{pmatrix}. \quad (3.2)$$

With the above quantities, the error in the estimated energy then propagates like:

$$\Delta E(\mathcal{C}) = \sqrt{(\nabla E)^T \text{COV}(a, b) \nabla E}. \quad (3.3)$$